BIOCHEMISTRY
including biophysical chemistry & molecular biology

Rapid Report

pubs.acs.org/biochemistry

# ATP Hydrolysis in the RecA–DNA Filament Promotes Structural Changes at the Protein–DNA Interface

Anna Reymer,[†] Sándor Babik,[‡] Masayuki Takahashi,[§] Bengt Nordén,[‡] and Tamás Beke-Somfai*[,‡,∥]

[†]Department of Chemistry and Molecular Biology, Gothenburg University, SE-405 30 Gothenburg, Sweden

[‡]Department of Chemical and Biological Engineering, Physical Chemistry, Chalmers University of Technology, SE-412 96 Gothenburg, Sweden

[§]School of Bioscience and Biotechnology, Tokyo Institute of Technology, 2-12-1-M6-14 Ookayama, Meguro-ku, Tokyo 152-8550, Japan

[∥]Institute of Materials Chemistry, Research Centre for Natural Sciences, Hungarian Academy of Sciences, Magyar tudósok krt. 2., H-1117 Budapest, Hungary

*S* *Supporting Information*

**ABSTRACT:** To address the mechanistic roles of ATP hydrolysis in RecA-promoted strand exchange reaction in homologous recombination, quantum mechanical calculations are performed on key parts of the RecA–DNA complex. We find that ATP hydrolysis may induce changes at the protein–DNA interface, resulting in the rearrangement of the hydrogen bond network connecting the ATP and the DNA binding sites.

DNA maintenance and repair are vital for normal cellular function; thus, all three kingdoms of life employ the process of homologous recombination reaction. A major element of this process is the exchange of strands between two homologous DNA molecules. In bacteria, genetic recombination is important also in horizontal gene transfer to propagate antibiotic resistance where RecA, an archetype enzyme, catalyzes the central step forming a DNA–protein complex in which DNA strands are compared and, in the case of sequence homology, exchanged.[1] ATP is involved in all recombinases, though its exact role is still unclear.

The strand exchange described above occurs in several steps. First, RecA monomers assemble onto a single-stranded DNA (ssDNA), with ATP binding between adjacent RecA monomers. This RecA–DNA–ATP filament[1,2] then also binds a double-stranded DNA (dsDNA), allowing screening for sequence homology between the two DNA molecules.[2] In the case of a homology match, strand exchange starts, and thereafter, the filament, now containing a newly formed dsDNA, dissociates into ssDNA, the new dsDNA, and ADP. ATP located between RecA monomers is hydrolyzed, and this may aid either the strand exchange reaction, the dissociation of the protein–DNA filamentous complex, or both.[3] X-ray structures of the DNA–RecA–ATP complex show that there is a H-bond network between DNA and ATP involving also Arg196, Gln194, and Glu96, the latter coordinating the $\gamma$-phosphate group in ATP (Figure 1).[1,4−6] When the filament size reaches 6–10 monomers, ATP hydrolysis starts and proceeds along the filament probably as a unidirectional wave, at a rate of 20–30 $min^{-1}$.[7,8]

However, how ATP hydrolysis may initiate and promote vital parts of this process remains elusive. To obtain atomic level insight, we here perform QM calculations on this reaction using large active site models that involve key regions at the RecA–RecA interfaces and the neighboring DNA strand.

We note that the problem of mechanochemical energy conversion coupled to ATP hydrolysis is also interesting in the context of other RecA-like helicases, such as PcrA, Rad50, Rho, and $F_oF_1$-ATP synthase.[9−11] These important biological energy converters show similarity both in macrostructural buildup and in how the ATP binding site is formed between subunits.[9] Recent computational advances and methodological progress make quantum mechanics/molecular mechanics (QM/MM) and active site QM methods useful for exploring protein function.[10,12−14] Here we employ QM models with more than 240 atoms, which can test the behavior of the larger environment near the reaction center. The QM models were built from a crystal structure in which $AlF_4$ and ADP were bound in the active site mimicking a transition state (TS) structure.[1] The models were constructed by closely investigating and comparing structural properties of RecA and ATP synthase active sites and using the software DOWSER,[15] which overall localized a total of five water molecules in the active site. The two models presented include key fragments of the active site, QM-I (196 atoms), and also parts connecting ATP with DNA, QM-II (245 atoms), where positions of some atoms were fixed to retain the structure of the active site (Figures S1 and S2). First, the T state was optimized and used for the other states as a reference. For validation, these were superimposed on the crystal structure, where no major differences were found (Figure S3). Calculations were performed at the B3LYP/6-311++G(d,p)//B3LYP/6-31G(d) level of theory with zero-point energy corrections and polarization effects of the protein considered. For more details on the models, see the Supporting Information.

We here focus on three key states of the reaction: ATP + $H_2O$ (T), ADP + $P_i$ (D), and a transition state (TS) in which

**Received:** June 4, 2015
**Revised:** July 20, 2015
**Published:** July 21, 2015





DOI: 10.1021/acs.biochem.5b00614
*Biochemistry* 2015, 54, 4579–4582

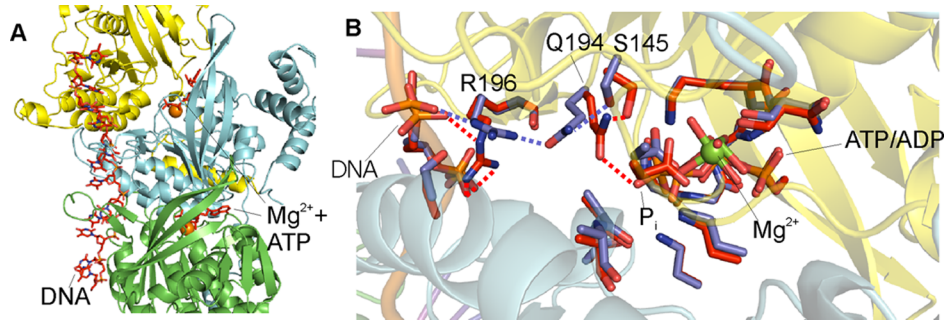


**Figure 1.** (A) RecA−ssDNA filament complex. Individual RecA units appear in different colors, and single-stranded DNA is shown as red sticks. ATP and $Mg^{2+}$ bind at interfaces of adjacent RecAs (ATP as red sticks, $Mg^{2+}$ as orange spheres). (B) Initial state, T (blue sticks), and end state $D_{Q,R\text{-}rot}$ (red sticks), in QM-II, superposed on the corresponding part of the RecA−DNA crystal structure (Protein Data Bank entry 3CMW).[1] Key residues connecting DNA and the ATP site are labeled, and selected H-bonds are shown as dotted lines. $Mg^{2+}$ is shown as a green sphere. From T to $D_{Q,R\text{-}rot}$, the H-bond breaks between side chains of Q194 and Arg196, and Arg196 could coordinate on the DNA. See the text and Table 1 for details.

the O−P bond in ATP breaks. In the initial T state, the optimized model has the triphosphate part of ATP surrounded by the Walker- or P-loop region, where the $\gamma$- and $\beta$-phosphates comprise an eclipsed configuration coordinated by $Mg^{2+}$ and Lys72 (Figure S1). Lys250 and Lys248 coordinate the same oxygen on $\gamma$-phosphate, with two H-bonds, the $O_\gamma\cdots H(\text{-}N)$ distances being 1.62 and 1.67 Å, respectively. The nucleophilic water is coordinated by the side chain of Glu96 and by an other O on the $\gamma$-phosphate.

Its oxygen, $O_W$, is 3.34 Å from the $\gamma$-phosphorus of ATP ($\gamma$P) (Figure 1 and Figure S1). This is in line with similar models and high-resolution crystal structures of related proteins.[16]

When the reaction moves from the T state to the bond-breaking TS state, the only major rearrangement observed is that Gln194 coordinates the nucleophilic water molecule, making a weak interaction with the lone orbital of the $NH_2$ group (Figure 1B and Figures S1 and S4).

The TS geometry has a planar $PO_3^-$ that was also observed in other ATPases.[17,18] Here the $O_W\cdots\gamma$P distance is 2.10 Å, while the $\gamma P\cdots O(\text{-}\beta P)$ distance is 2.71 Å, which is somewhat longer than those of observed for the other enzymes.

In the final ADP + $P_i$ state, the $P_i$ is doubly protonated and forms H-bonds with an oxygen of the $\beta$-phosphorus in ADP and with the nitrogen from the CO-$NH_2$ group of the Gln194 side chain. In crystal structures, the carbonyl oxygen from this CO-$NH_2$ group is H-bonded to the positively charged guanidinium group of Arg196, which is located between the ATP site and DNA in the protein. This leaves the $NH_2$ part of the group pointing toward the ATP site. However, another orientation has also been found, where the carbonyl group is turned toward the active site.[1] In a related manner, we note that several of our initial calculations resulted in such a rotated position during the development of model QM-I. Note that Gln194 and Arg196 are believed to be key residues implicated in allosteric coupling of DNA binding to ATP binding.[3,19]

Therefore, to assess the potential role of Gln194 side chain positioning, the same states were also located with the carbonyl group on Gln194 rotated toward the ATP site (i.e., $T_{Q\text{-}rot}$, $TS_{Q\text{-}rot}$, and $D_{Q\text{-}rot}$). In $T_{Q\text{-}rot}$, the active site is very similar to the T state, though the nucleophilic water in $T_{Q\text{-}rot}$ is coordinated via the C=O group of the Gln194 side chain. The difference between TS and $TS_{Q\text{-}rot}$ is more pronounced as for the latter the $O_w\cdots\gamma$P (2.08 Å) and $\gamma P\cdots O(\text{-}\beta P)$ (2.56 Å) distances are shorter (Figures S1 and S4). Further, in $D_{Q\text{-}rot}$, a new H-bond is formed between the Gln194 carbonyl and the H-(O-) group of the $P_i$ (Figure 2 and Figure S4).

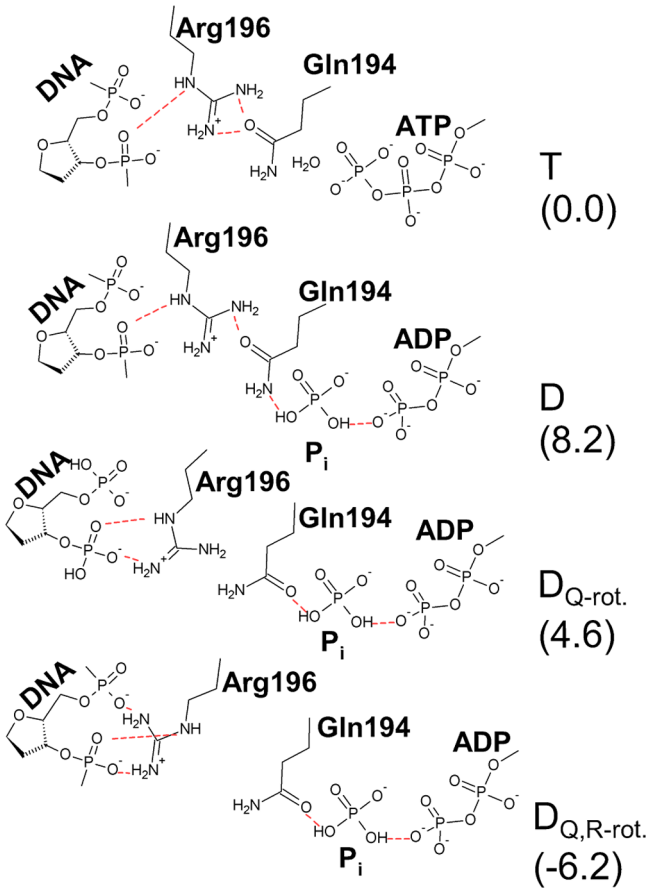


**Figure 2.** Schematics of the H-bond network (dashed red lines) and its changes along the reaction steps (QM-II relative energies in kilocalories per mole in parentheses). For more details, see Figure S5.

Considering energies of the six conformations obtained in QM-I described above (Table 1 and Figure 2), the barrier height of hydrolysis in the original conformation is 27.9 kcal/mol. The D state is slightly less favored than the T state, by 3.5 kcal/mol. In contrast, in the Q-rot state, both the $TS_{Q\text{-}rot}$ and $D_{Q\text{-}rot}$ states are stabilized relative to the T state (Table 1), which results a lower barrier, 23.6 kcal/mol. This value is in the vicinity of the experimental hydrolysis rate, derived back to a free energy of 18 kcal/mol using classical transition state theory. The accuracy of QM active site models was earlier estimated to be relatively good, with errors of a few kilocalories



DOI: 10.1021/acs.biochem.5b00614
*Biochemistry* 2015, 54, 4579−4582

Table 1. Relative Energies of Selected Key Reaction Steps[a]

| reaction step | | QM-I[b] | QM-II[c] |
|---|---|---|---|
| | initial state | | |
| ATP + $H_2O$ | T | 0.0 | 0.0 |
| TS ($PO_3^-$) | TS | 27.9 | |
| ADP + $P_i$ | D | 3.5 | 8.2 |
| | Gln194 rotated | | |
| ATP + $H_2O$ | $T_{Q\text{-rot}}$ | 8.8 (0.0)[d] | 8.9 |
| TS ($PO_3^-$) | $TS_{Q\text{-rot}}$ | 23.6 (14.7) | |
| ADP + $P_i$ | $D_{Q\text{-rot}}$ | 0.3 (−8.5) | 4.6 |
| | Arg196 rotated | | |
| ADP + $P_i$ | $D_{Q,R\text{-rot}}$ | | −6.2 |

[a]All values are in kilocalories per mole. Please see the Supporting Information for more details. [b]Obtained at the B3LYP/6-311++G(d,p)//B3LYP/6-31G(d) level of theory. [c]Obtained at the B3LYP/6-31+G(d,p)//B3LYP/6-31G(d,p) level of theory. [d]Values in parentheses are given using $T_{Q\text{-rot}}$ as a reference.

per mole, which does not affect significantly the conclusions drawn here.[13]

To address the mechanistic role of ATP hydrolysis in the complex, we used an extended model, QM-II. The rotated Gln194 side chain would break up the H-bond with Arg196; thus, we focused on this residue: QM-II included all heavy polar neighboring groups of the Arg196 side chain and also a fragment of the DNA strand (Figures 1 and 2 and Figure S5). In QM-II, the T and D states were obtained for both the original and rotated position of the Gln194 side chain (Table 1 and Figure 2). While the active site conformations of these states are rather similar in QM-I and QM-II, the latter reveals that in the Q-rot states the Arg196 side chain has a larger distance to Gln194 and coordinates closer to DNA. This is even more pronounced in $D_{Q\text{-rot}}$, where the Arg196 side chain is in an optimal position to coordinate the two negative phosphates of the DNA−sugar−phosphate backbone (Figure 2). This results in a state in which both Gln194 and Arg196 side chains are rotated from their original positions ($D_{Q,R\text{-rot}}$), which is significantly stabilized, by 6.2 kcal/mol, relative to the initial T (Table 1).

Upon comparing relative energies of the T, D, $T_{Q\text{-rot}}$, and $D_{Q\text{-rot}}$ states in QM-II with those obtained in QM-I, we note smaller shifts in values, but the overall qualitative differences remain the same. The T state is somewhat favored over D in the original Gln194 side chain position, whereas the $D_{Q\text{-rot}}$ state is favored over $T_{Q\text{-rot}}$. The large CPU requirements set by a QM system with 245 atoms allowed us to focus on only selected states, and thus, the TS in QM-II was not obtained. Nevertheless, compared to QM-I, QM-II did not have additional groups near the $O_w\cdots\gamma P\cdots O(\text{-}\beta P)$ region, and in such cases, the TS barrier height is not expected to change significantly.[17] The energetic variations between T-TS-D and $T_{Q\text{-rot}}$-$TS_{Q\text{-rot}}$-$D_{Q\text{-rot}}$ obtained are quite similar when compared to those of the $F_1$-ATPase mechanism.[20,21] In the case of $F_1$-ATPase, the decrease in barrier height at the TS and the stabilization of the D state occur when the so-called "tight" ATP binding site conformation converts to a "loose" conformation coupled to a 120° rotation of the central $\gamma$-subunit. Recently, Ma et al. have shown that the Rho−RNA complex has an ATP-coupled force generation mechanism very similar to that of the latter.[11] These suggest that beside similarities in macroscopic buildup, this protein family may also have several common mechanistic elements, including the ATP hydrolysis reaction and its coupling to the substrate site through a H-bond network.

We have addressed ATP hydrolysis at the RecA−RecA interface in the RecA−DNA filament complex, using large active site QM models. Important conformational changes triggered by ATP hydrolysis would induce a new orientation of the Arg196 side chain, bringing it right next to the DNA backbone gap region. This new coordination may change the stability of the RecA−DNA complex. The observed flipping of Arg196 in RecA seems to be very similar to the conformational change of Lys326 inside the translocation channel of Rho transcription termination factor.[11] Both of these residues flip toward and away from their corresponding substrates, controlled by ATP hydrolysis and ATP binding. This mechanism provides a plausible scenario for RecA for the early stages of the filament disassembly and release of the newly formed duplex, as well as generation of some torsional freedom needed to accomplish the strand exchange step. The idea that the filament disassembly results from cooperation between ATP hydrolysis and release of the tension is supported by single-molecule experiments, which show that external tension applied to the DNA slows filament disassembly.[22] A similar trend is also observed in the case of eukaryotic recombinase Rad51.[23] Our QM results give useful atomic level insight into how ATP hydrolysis initiates important conformational changes, which are in good accord with the experimental observations described above. However, to reach solid conclusions about the macroscopic mechanism and to understand how the Arg196−DNA interaction affects the complex, larger scale models capable of reporting on protein−DNA level rearrangements initiated by ATP hydrolysis will also be required.[11] Currently, such models are subject to investigation in our laboratory.

## ■ ASSOCIATED CONTENT

### Supporting Information

The Supporting Information is available free of charge on the ACS Publications website at DOI: 10.1021/acs.biochem.5b00614.

Computational details as well as details about the structural properties of the located critical points in the QM models (PDF)

## ■ AUTHOR INFORMATION


### Corresponding Author

*E-mail: beke@chalmers.se. Phone: +3613826624.



### Funding

A.R. was funded by Swedish Research Council VR Grant 637-2014-437.


### Notes

The authors declare no competing financial interest.

## ■ REFERENCES


(1) Chen, Z. C., Yang, H. J., and Pavletich, N. P. (2008) Mechanism of homologous recombination from the RecA-ssDNA/dsDNA structures. *Nature* 453, 489−U483.

(2) Bianco, P. R., Tracy, R. B., and Kowalczykowski, S. C. (1998) DNA strand exchange proteins: a biochemical and physical comparison. *Front Biosci* 3, D570−603.

(3) Bell, C. E. (2005) Structure and mechanism of Escherichia coli RecA ATPase. *Mol. Microbiol.* 58, 358−366.




DOI: 10.1021/acs.biochem.5b00614
*Biochemistry* 2015, 54, 4579−4582

(4) Rajan, R., and Bell, C. E. (2004) Crystal structure of RecA from Deinococcus radiodurans: Insights into the structural basis of extreme radioresistance. *J. Mol. Biol. 344*, 951−963.
(5) Xing, X., and Bell, C. E. (2004) Crystal structures of Escherichia coli RecA in a compressed helical filament. *J. Mol. Biol. 342*, 1471−1485.
(6) Cox, J. M., Abbott, S. N., Chitteni-Pattu, S., Inman, R. B., and Cox, M. M. (2006) Complementation of one RecA protein point mutation by another - Evidence for trans catalysis of ATP hydrolysis. *J. Biol. Chem. 281*, 12968−12975.
(7) Cox, J. M., Tsodikov, O. V., and Cox, M. M. (2005) Organized unidirectional waves of ATP hydrolysis within a RecA filament. *PLoS Biol. 3*, e52.
(8) Bakhlanova, I. V., Dudkina, A. V., and Baitin, D. M. (2013) Enzymatic control of homologous recombination and hyperrecombination in Escherichia coli. *Mol. Biol. 47*, 181−191.
(9) Ye, J. Q., Osborne, A. R., Groll, M., and Rapoport, T. A. (2004) RecA-like motor ATPases - lessons from structures. *Biochim. Biophys. Acta, Bioenerg. 1659*, 1−18.
(10) Dittrich, M., Yu, J., and Schulten, K. (2007) PcrA helicase, a molecular motor studied from the electronic to the functional level. *Atomistic Approaches in Modern Biology 268*, 319−347.
(11) Ma, W., and Schulten, K. (2015) Mechanism of Substrate Trans location by a Ring-Shaped ATPase Motor at Millisecond Resolution. *J. Am. Chem. Soc. 137*, 3031−3040.
(12) Warshel, A. (1997) *Computer modeling of chemical reactions in enzymes and solutions*, Wiley professional paperback series, pp *xiv*, 236, Wiley, New York.
(13) Noodleman, L., Lovell, T., Han, W. G., Li, J., and Himo, F. (2004) Quantum chemical studies of intermediates and reaction pathways in selected enzymes and catalytic synthetic systems. *Chem. Rev. 104*, 459−508.
(14) Senn, H. M., and Thiel, W. (2007) QM/MM methods for biological systems. *Atomistic Approaches in Modern Biology 268*, 173−290.
(15) Zhang, L., and Hermans, J. (1996) Hydrophilicity of cavities in proteins. *Proteins: Struct., Funct., Genet. 24*, 433−438.
(16) Menz, R. I., Walker, J. E., and Leslie, A. G. W. (2001) Structure of bovine mitochondrial Fl-ATPase with nucleotide bound to all three catalytic sites: Implications for the mechanism of rotary catalysis. *Cell 106*, 331−341.
(17) Beke-Somfai, T., Lincoln, P., and Norden, B. (2011) Double-lock ratchet mechanism revealing the role of alpha SER-344 in F(o)F(1) ATP synthase. *Proc. Natl. Acad. Sci. U. S. A. 108*, 4828−4833.
(18) Beke-Somfai, T., Lincoln, P., and Norden, B. (2013) Rate of hydrolysis in ATP synthase is fine-tuned by alpha-subunit motif controlling active site conformation. *Proc. Natl. Acad. Sci. U. S. A. 110*, 2117−2122.
(19) Kelley, J. A., and Knight, K. L. (1997) Allosteric regulation of RecA protein function is mediated by Gln(194). *J. Biol. Chem. 272*, 25778−25782.
(20) Yang, W., Gao, Y. Q., Cui, Q., Ma, J., and Karplus, M. (2003) The missing link between thermodynamics and structure in F1-ATPase. *Proc. Natl. Acad. Sci. U. S. A. 100*, 874−879.
(21) Beke-Somfai, T., Lincoln, P., and Norden, B. (2010) Mechanical Control of ATP Synthase Function: Activation Energy Difference between Tight and Loose Binding Sites. *Biochemistry 49*, 401−403.
(22) van Loenhout, M. T. J., van der Heijden, T., Kanaar, R., Wyman, C., and Dekker, C. (2009) Dynamics of RecA filaments on single-stranded DNA. *Nucleic Acids Res. 37*, 4089−4099.
(23) van Mameren, J., Modesti, M., Kanaar, R., Wyman, C., Peterman, E. J. G., and Wuite, G. J. L. (2009) Counting RAD51 proteins disassembling from nucleoprotein filaments under tension. *Nature 457*, 745−748.



DOI: 10.1021/acs.biochem.5b00614
*Biochemistry* 2015, 54, 4579−4582